Tunable swelling and deswelling of temperature- and light-responsive graphene oxide-poly(N-isopropylacrylamide) composite hydrogels

Journal:	*Polymer Chemistry*
Manuscript ID	PY-COM-12-2019-001934.R1
Article Type:	Communication
Date Submitted by the Author:	25-Feb-2020
Complete List of Authors:	Li, Minghao ; University of California San Diego, Materials Science and Engineering Program Bae, Jinhye; University of California San Diego, Department of NanoEngineering

COMMUNICATION

Tunable swelling and deswelling of temperature- and light-responsive graphene oxide-poly(N-isopropylacrylamide) composite hydrogels

Received 00th January 20xx,
Accepted 00th January 20xx

DOI: 10.1039/x0xx00000x

Minghao Li[a] and Jinhye Bae*[a,b,c]

Tunable swelling and deswelling behaviors of graphene oxide-poly(N-isopropylacrylamide) (GO-PNIPAM) composite hydrogels are demonstrated by controlling the internal microstructures and the rate of external temperature change. The different internal microstructures of GO-PNIPAM composite hydrogels as a function of concentrations of GO and chemical crosslinker explain their different swelling and deswelling ratios. Furthermore, the light-driven shape deformation of GO-PNIPAM is demonstrated by utilizing the photothermal property of GO. This approach offers promise for light and temperature-responsive actuators and sensors, and biomedical applications.

Stimuli-responsive hydrogels have three-dimensional elastic networks composed of cross-linked hydrophilic polymer chains which can absorb a large amount of water, and undergo significant volume or other physiochemical properties changes in response to various external stimuli such as temperature,[1] pH,[2] electric field,[3] light[4, 5] and chemicals.[6, 7] The stimuli-responsive systems have provided promising applications in biosensors,[8] smart actuators,[9] and biomimetic systems.[10, 11] Among various stimuli-responsive hydrogels, crosslinked poly(N-isopropylacrylamide) (PNIPAM) is one of the well-known temperature-responsive materials, exhibiting a low critical solution temperature (LCST) in a range from 30 to 50 °C that could be adjusted by the molecular weight and end group polarity.[12-14] When the temperature is above LCST, PNIPAM hydrogels undergo a reversible hydrophilic-to-hydrophobic property change as a result of the transition from the hydrated (*i.e.*, swelled) state to dehydrated (*i.e.*, deswelled) state.[15] Although PNIPAM hydrogels have been heavily studied, there are still a couple of remaining limitations including the relatively slow kinetics of their shape morphing and their low mechanical toughness.[16-18] Programming multiple shape changes as well as overcoming these limitations are critical for exploring practical applications of the PNIPAM hydrogel systems. Hence, photothermal materials (*e.g.*, gold nanoparticles,[19] carbon nanotubes,[20] iron oxide (Fe_3O_4) nanoparticles[21] and graphene oxide sheets (GO)[22]) have drawn great attention as an additive since they are able to achieve the shape reconfiguration on a relatively fast time scale,[16, 23] the additive-enhanced toughness[24, 25] and the triggering of shape deformations by local light irradiation.[25] Specifically, photothermal materials embedded in a temperature-responsive hydrogel network (*i.e.*, a photothermal composite hydrogel) have the capability to absorb light and generate heat. Thereby, such heat induces the temperature rise (> LCST) in the thermally responsive hydrogel networks and triggers their volume changes.[26] Photothermal composite hydrogels offer promising potential in various applications where fast or controllable response kinetics is necessary such as drug delivery system,[27] smart microvalves,[26] switches,[28] and grippers.[29]

Among the various photothermal materials, GO provides unique aspects compared to other nano and microparticles because GO is a two-dimensional (2D) single-atomic carbon thin sheet, thus has a high area-to-edge ratio with a lateral size of ~0.1 – 10 μm and a thickness of 1 nm.[30] Moreover, it has cytotoxicity and amphiphilicity.[31-34] This amphiphilicity of GO is derived since the basal plane of GO is more hydrophobic due to the π-conjugation domains,[35] whereas the edge of GO is more hydrophilic owing to polar oxygen functional groups.[30] Due to these unique features, GO has been utilized as a functional additive in PNIPAM hydrogels. For example, the GO-PNIPAM composite system has been demonstrated as switchable glazing by absorbing sunlight for adaptive solar control windows,[36] controllable and reversible shape variations under near-infrared (NIR) light exposure,[25, 37] and a reinforcement additive to enhance the mechanical properties of PNIPAM hydrogels.[24] The excellent stability of GO additives in PNIPAM hydrogels is due to the interactions with PNIPAM networks. Specifically, PNIPAM chains and GO can be

[a]*Materials Science and Engineering Program, University of California San Diego, La Jolla, CA 92093, United States.*
[b]*Department of NanoEngineering, University of California San Diego, La Jolla CA 92093, United States*
[c]*Chemical Engineering Program, Department of Nanoengineering, University of California San Diego, La Jolla, CA 92093, United States*
†Electronic Supplementary Information (ESI) available: Experimental sections, Tables and characterization. See DOI: 10.1039/x0xx00000x

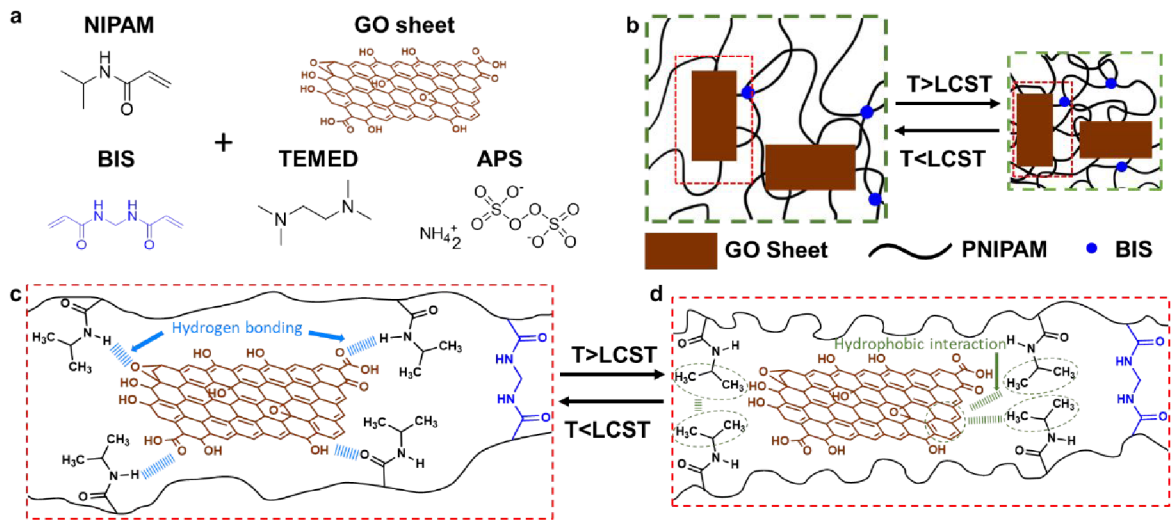

Figure. 1. Schematic illustration of fabrication and swelling/deswelling mechanism of GO-PNIPAM composite hydrogels. (a) Synthesis of crosslinked GO-PNIPAM composite hydrogels. (b) Temperature-responsive expanding and collapsing of PNIPAM networks in the swelling and deswelling states of GO-PNIPAM, respectively. Reversible change of predominant interactions between hydrogen bonding and hydrophobic interaction across PNIPAM networks and GO by temperature (c) below and (d) above LCST, respectively.

physically crosslinked by hydrogen bonding, and residual C=C bonds on the basal plane of GO can possibly be grafted with PNIPAM chains as covalent interactions.[38, 39] Therefore, we hypothesize both the loading concentration of GO and the degree of chemical crosslinking of hydrogel networks could affect the overall microstructure, thus the swelling and deswelling behaviors of GO-PNIPAM composite hydrogels. Understanding their microstructure-dependent swelling/deswelling behaviors can be crucial for design stimuli-responsive 3D shape morphing and actuation, and their practical applications. To date, however, the swelling/deswelling behaviors of GO-PNIPAM composite hydrogel systems have not been explored yet in terms of the rate of external temperature change with different chemical and physical crosslinking densities of GO-PNIAPM.

Here, we demonstrate the tunable swelling and deswelling properties of GO-PNIPAM composite hydrogels with different concentrations of GO and chemical crosslinker as well as different rates of cooling and heating. GO-PNIPAM composite hydrogels are fabricated with different concentrations of GO (flake size: 0.5 - 5 μm) as 2D micro-additives and N,N'-methylenebisacrylamide (BIS) as the chemical crosslinker,[24] and their degree of swelling and deswelling are characterized by different rates of cooling and heating. Notably, a "non-shrinkable" deswelling behavior is observed at a certain range of GO loading concentrations by the fast heating rate (*i.e.*, non-equilibrium condition). Internal microstructures of these composite hydrogels with different GO and BIS concentrations at the swelled and deswelled states are characterized by scanning electron microscope (SEM), optical microscope (OM) and atomic force microscope (AFM). In addition, GO-PNIPAM thin sheets with different GO concentrations are used to demonstrate photothermal shape actuation by UV irradiation.

Fig. 1 illustrates the single-step preparation of GO-PNIPAM composite hydrogels consisting of free radical polymerization by N,N,N',N'-tetramethylethylenediamine (TEMED) as an accelerator and 10 wt% aqueous ammonium persulfate (APS) as an initiator, and chemical crosslinking by BIS as a crosslinker (Fig. 1a),[17] the temperature-responsive expanding and collapsing of PNIPAM networks in the swelling and deswelling states of GO-PNIPAM, respectively (Fig. 1b), and reversible switching of the predominant interactions between GO and PNIPAM networks by temperature change (Fig. 1c and d). When the temperature is below LCST, hydrophilic amine groups in PNIPAM chains reorient and extend in order to form hydrogen bonds with surrounding water molecules and oxygen-containing groups on GO as the swelled state (Fig. 1c). However when the temperature increases above the LCST, the hydrophobic interaction between isopropyl groups increases because the intrinsic affinity of polymer chains enhances (Fig. 1d), which means that crosslinked PNIPAM chains change from an extended coil to a fully collapsed chain globule (*i.e.*, the coil-to-globule transition), thereby the networks will collapse (Fig. 1b).[40, 41]

To better understand the temperature-dependent conformation of PNIPAM networks and interactions between GO and PNIPAM chains, we characterized the linear swelling ratio λ_s and the linear deswelling ratio λ_d of GO-PNIPAM with different BIS and GO concentrations under different temperatures (Fig. 2). GO-PNIPAM samples were biopsy-punched into a thin disk shape with a diameter of 3 mm and a thickness of 1 mm in the as-prepared state. The linear swelling ratio λ_s is defined as D_s/D_0, where D_s and D_0 are the equilibrium diameters of a thin hydrogel disk at 23 °C and the as-prepared state, respectively. Linear deswelling ratio λ_d is defined as D_d/D_0, where D_d represents the equilibrium diameter of a thin hydrogel disk at 49 °C. The composite hydrogels were

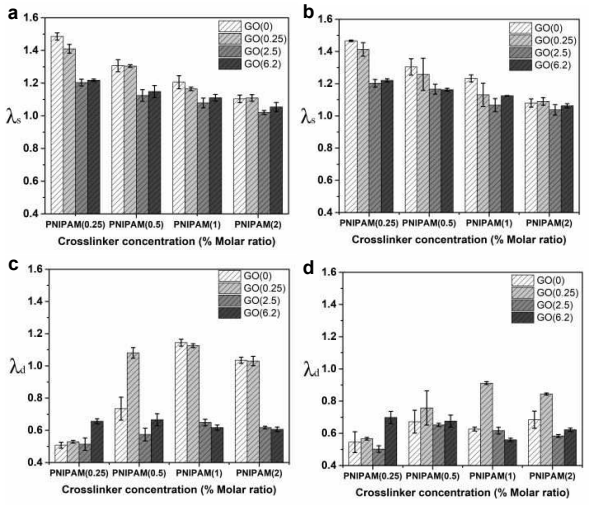

Figure. 2. Linear swelling ratio λ_s for GO-PNIPAM composite hydrogels when (a) external temperature decreasing gradually with 2 °C/hour from 49 to 23 °C; and (b) external temperature decreasing abruptly from 49 to 23 °C. Linear deswelling ratio λ_d for GO-PNIPAM composite hydrogels when (c) external temperature increasing abruptly from 23 to 49 °C; and (d) external temperature increasing gradually with 2 °C/hour from 23 to 49 °C.

designated as "GO(*x*)-PNIPAM(*y*)", where "*x*" represents the concentration of GO (mg mL^{-1}), "*y*" indicates the percentage molar ratio of BIS to NIPAM (%) in a batch solution (Table S1†). For example, GO(2.5)-PNIPAM(1) was prepared by a batch solution containing GO with a concentration of 2.5 mg mL^{-1} and a molar ratio of BIS to NIPAM equivalent to 1%. The temperature range between 23 to 49 °C for swelling/deswelling tests was determined by linear swelling ratio (λ) curve of GO-PNIPAM as a function of temperature (Fig. S1†). This curve exhibited the difference of λ at 49 °C and 61 °C is less than 1%. Optical microscopy (Nikon, Eclipse LV100N POL) was used to measure the sample size upon abrupt temperature change (*i.e.*, fast heating rate), the hydrogel disks swelled in water at 23 °C and were immediately transferred into 49 °C water. Their sizes were measured after 1-hour immersion at 49 °C and 24-hour immersion at 23 °C. For gradual temperature change (*i.e.*, slow heating rate), the sample size was measured in the range from 23 to 49 °C with increasing/decreasing of 2 °Cover 15 min and subsequently holding 1-hour for stabilization.

Both BIS and GO concentrations affect λ_s of the GO-PNIPAM composite hydrogels (Table S2†). λ_s of samples with the fixed GO concentration decreases as BIS molar ratio (*y*) increases from 0.25 to 2 mol%. It indicates that increasing the degree of chemical crosslinking suppresses the swelling of the hydrogels. Similarly, λ_s of the GO-PNIPAM decreases overall when GO loading (*x*) increases from 0 to 2.5 mg mL^{-1} at the fixed BIS concentration. This trend reveals that GO can serve a similar role as the BIS crosslinker due to the presence of hydrogen bonding and covalent interactions between GO and PNIPAM chains.[24, 38] For composite hydrogels with 6.2 mg mL^{-1} GO loading, they exhibit an average of ~ 3 % increasing of λ_s than GO(2.5)-PNIPAM composite hydrogels while λ_s decreases an average of ~ 10 % when GO concentration increases from 0 to 2.5 mg mL^{-1}. Since the spacing between GO sheets tends to decrease at relatively high GO loading (*i.e.*, 6.2 mg mL^{-1}), there is a higher probability to form hydrogen bonding and intermolecular interaction between GO and GO.[42-44] We hypothesize when GO concentration increases from 2.5 to 6.2 mg mL^{-1}, the effective number of physical crosslinking (*i.e.*, hydrogen bonding) between GO and PNIPAM networks is lowered due to the increasing probability of GO-GO interactions, thus, resulting in the increment of λ_s. Swelling by gradual (Fig. 2a) and abrupt cooling (Fig. 2b) leads to similar values of λ_s for the GO-PNIPAM composite hydrogels. This means that λ_s is mostly affected by the final temperature rather than the rate of cooling. Swelling by gradual (Fig. 2a) and abrupt cooling (Fig. 2b) leads to similar values of λ_s for the GO-PNIPAM composite hydrogels. This means that λ_s is mostly affected by the final temperature rather than the rate of cooling.

Next, we investigated the deswelling behaviors of GO-PNIPAM composite hydrogels. PNIPAM with 0 and 0.25 mg mL^{-1} GO show relatively a larger λ_d (*i.e.*, a lesser degree of deswelling) upon abrupt heating compared to PNIPAM with 2.5 and 6.2 mg mL^{-1} GO concentrations (Fig. 2c). Specifically, GO(0)-PNIPAM(1) (λ_d = 1.14) and GO(0.25)-PNIPAM(1) (λ_d = 1.13) exhibit much less deswelling than GO(2.5)-PNIPAM(1) (λ_d = 0.65) and GO(6.2)-PNIPAM(1) (λ_d = 0.62) under abrupt heating from 23 °C to 49 °C. We suspect this unique deswelling behavior (λ_d > 1) to arise from the different timescales between heat and water diffusions. The characteristic thermal diffusivity of the hydrogels is ~10^{-7} m^2 s^{-1},[45] and the poroelastic diffusion constant for PNIPAM hydrogels is ~10^{-11} m^2 s^{-1}.[18, 46] Regarding a 1 mm thick hydrogel disk, the theoretical timescale for thermal diffusion should be ~4 seconds, whereas the poroelastic timescale could be ~27 hours for swelling/deswelling. Therefore, we hypothesize that the higher λ_d of hydrogels is possibly caused by the formation of a dense outermost layer of collapsed PNIPAM networks at the initial stage of deswelling due to the abrupt temperature change to 49 °C. The formation of the dense outermost layer could effectively suppress the outward water flux from the hydrogel.[47-50] Although the theoretical equilibrium time for hydrogel swelling/deswelling is in the order of 10 hours, we experimentally tested the required time period to reach the equilibrium swelling/deswelling state. We determined the required immersion time to measure λ_s at 23 °C and λ_d at 49 °C are 24 and 1 hour, respectively. Note that the observed difference in λ_d after 1- and 6-hour immersions at 49 °C was less than 3 %.

We next explored the deswelling behaviors of GO-PNIPAM composite hydrogels under gradual heating (Table S2†). Interestingly, the PNIPAM with 0 and 0.25 mg mL^{-1} GO were significantly deswelled thus measured λ_d decreases more than 20 % relative to λ_d by abrupt heating, whereas the PNIPAM with 2.5 and 6.2 mg mL^{-1} GO exhibited less than 7 % difference in λ_d between abrupt and gradual heating processes (Fig. 2d). These results imply that the relatively higher GO loading within the PNIPAM networks could significantly slow down or even may prevent the formation of dense outermost layer by collapsing hydrogel networks upon deswelling. Thereby, water

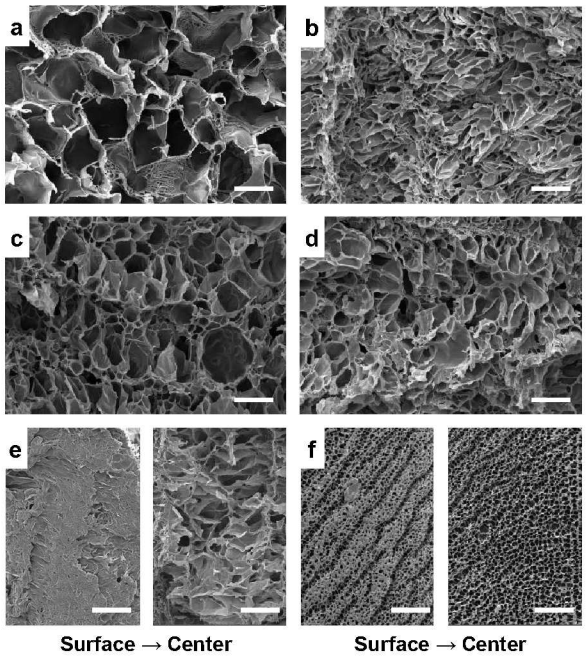

Figure. 3. SEM micrographs of swelled samples at 23 °C, (a) GO(0)-PNIPAM(0.25); (b) GO(0)-PNIPAM(2); (c) GO(6.2)-PNIPAM(0.25); (d) GO(6.2)-PNIPAM(2), deswelled samples at 49 °C near the surface and the center of (e) GO(0.25)-PNIPAM(2); (f) GO(6.2)-PNIPAM(2). Scale bar = 25 μm.

can continuously flow out from the interior of the hydrogels. In addition, we tested the reversibility of these deswelling behaviors depending on GO concentrations by repeating multiple cycles of abrupt heating and cooling. The measured swelling/deswelling ratios (λ) for each GO concentration are well reproducible up to 5 cycles of the abrupt heating and cooling. (Fig. S2†). Notably, in the case of GO(0)-PNIPAM(1) and GO(0.25)-PNIPAM(1), the differences in λ between swelling at 23 °C and deswelling at 49 °C were less than 10%, and such unique deswelling behaviors ($\lambda_d > 1$) are fully reversible and repeatable upon the heating-cooling cycles.

We further explored the swelling and deswelling behaviors for GO-PNIPAM with different compositions of GO and BIS by weight swelling ratio, $\eta = (W_T - W_{dry})/ W_{dry}$, where W_T is the weight of composite hydrogel at either 23 or 49 °C for fully swelling and deswelling, respectively, and Wdry is the weight of the dried hydrogel. The values of η indicate the water absorption ability per unit hydrogel weight. We note that the weight of GO within GO(6.2)-PNIPAM is less than 6 wt% relative to the entire GO-PNIPAM weight thus the weight contribution of GO is trivial. We measured η at 23 and 49 °C for the swelled and deswelled state by abrupt temperature change of GO-PNIPAM (Fig. S3†). The result reveals that η for PNIPAM(1) and PNIPAM(2) composite hydrogels have an overall similar trend with λ_s and λ_d in Fig. 2b and c. For instance, a higher concentration of GO lead to lower η but GO(6.2)-PNIPAM showed increased η at 23 °C than GO(2.5)-PNIPAM. At 49 °C, PNIPAM with GO(0) and GO(0.25) exhibited a larger η than PNIPAM with high concentrations of GO, GO(2.5) and GO(6.2).

To consider the correlation between swelling/deswelling behaviors and their internal structures of GO-PNIPAM with different GO and BIS concentrations, we characterized the internal microstructures of freeze-dried GO-PNIPAM by SEM. The porous microstructures in the freeze-dried GO-PNIPAM result from the water-to-ice transformation during freezing and hydrogel networks serve as templates for pore formation.[51] We found that the pore size of the internal microstructure (Table S3†) of the swelled samples is related to both the concentrations of GO and BIS (Fig. 3a to d). PNIPAM hydrogels without GO, GO(0)-PNIPAM(0.25) and GO(0)-PNIPAM(2), reveal pores of 27.9 ± 2.3 and 6.3 ± 3.2 μm in diameter, respectively (Fig. 3a and b). Thus, this trend of pore size as a function of BIS agrees that the greater swelling ratios result from lower BIS concentrations (Fig. 3a and b). However, when a significant amount of GO was added with lower BIS (*i.e.*, GO(6.2)-PNIPAM(0.25), Fig. 3c), much smaller internal pores with diameters of 11.5 ± 7.5 μm formed due to the presence of hydrogen bonding and covalent interactions between GO and PNIPAM networks which could serve as additional crosslinking.[24, 39] GO(6.2)-PNIPAM(2) (7.3 ± 3.6 μm in diameter, Fig. 3d) shows only a small increment in average pore size but overall reveals a similar porous structure compared with GO(0)-PNIPAM(2). We suspect that the pore size (*i.e.*, mesh size) of highly crosslinked PNIPAM networks in the swelled state is already close to GO flake size (~5 μm), GO may have less effect on the overall porous structures. Moreover, GO(0.25)-PNIPAM(0.25) (23.3 ± 3.9 μm in diameter, Fig. S4a†) and GO(0.25)-PNIPAM(2) (6.6 ± 3.2 μm in diameter, Fig. S4b†) shows a similar pore size with GO(0)-PNIPAM(0.25) and GO(0)-PNIPAM(2), respectively. It means that BIS concentration is more dominant in determining their microstructures when GO concentration is relatively low.

Fig. 3e exhibits the microstructures of the deswelled GO(0.25)-PNIPAM(2) taken close to the surface and center of the sample. The SEM image near the surface (Fig. 3e, left) shows dense and collapsed structures, and it clearly supports our hypothesis that abrupt heating leads to the formation of a dense polymer outermost layer on the hydrogel disk in the initial stage of deswelling. Whereas, the SEM image from the central area of the deswelled GO(0.25)-PNIPAM(2) (Fig. 3e, right) shows a

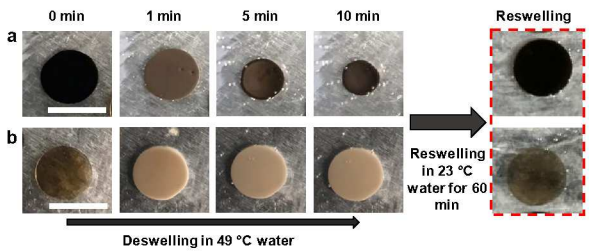

Figure. 4. Photographs of temperature-responsive characteristics of (a) GO(2.5)-PNIPAM(1) and (b) GO(0.25)-PNIPAM(1) composite hydrogels when external temperature abruptly changes from 23 to 49 °C (0 min) and after 1, 5, and 10 min at 49 °C. After 10 min, hydrogels reswell in water at 23 °C for 60 min. Swelling medium is DI water. Scale bar is 1

similar pore size (6.6 ± 3.4 μm in diameter) to the sample in the swelled state. Such microstructural differences between near the surface and the center of the deswelled GO-PNIPAM explains the unusual deswelling behaviors (*i.e.*, $\lambda_d > 1$). On the other hand, the deswelled GO(6.2)-PNIPAM(2) (Fig. 3f) reveals the similarity in porous microstructure between near the surface (2.4 ± 1.3 μm in diameter) and the center of the sample (2.1 ± 1.3 μm in diameter). Therefore, we verified that the high loading concentration of GO led to form more uniform porous structures throughout the sample, and prevented to form the dense outermost layer. Further, it reasonably explains much greater degree of deswelling of GO(6.2)-PNIPAM(2) (*i.e.*, λ_d = 0.61) as opposed to GO(0.25)-PNIPAM(2) (*i.e.*, λ_d = 1.03). To further characterize the surface topologies of deswelled GO-PNIPAM, OM and AFM images of the deswelled and freeze-dried samples were observed. These results also prove the different surface topologies between GO(0.25)-PNIPAM(2) and GO(6.2)-PNIPAM(2) at the deswelled state (Fig S5†). The OM images show a smooth surface of GO(0.25)-PNIPAM(2) and a porous surface texture of GO(6.2)-PNIPAM(2). The AFM height profile of GO(6.2)-PNIPAM(2) exhibits a much greater surface height different (1.47 μm) with a steeper cross-sectional profile compared to GO(0.25)-PNIPAM(2).

We next visually demonstrated how the formation of a dense polymer outermost layer affects deswelling of GO(0.25)-PNIPAM(1) (*i.e.*, λ_d = 1.13) and GO(2.5)-PNIPAM(1) (*i.e.*, λ_d = 0.65) at 49 °C as a function of time after abrupt heating (Fig. 4). Samples for each composition were fully swelled in deionized water for 72 hours at 23 °C to reach the equilibrium state. Then they were biopsy-punched into a thin disk shape with a diameter of 10 mm and a thickness of 1 mm. Within 1 min at 49 °C, both sample disks change from transparent to opaque, thus reach the cloud point of PNIPAM hydrogels[52] before shrinking the disks. After 1 min at 49 °C, GO(2.5)-PNIPAM(1) disk continues to shrink up to 10 min and stabilizes in size, whereas GO(0.25)-PNIPAM(1) disk almost preserves its swelled size while maintaining the opaque color. Both composite hydrogel disks can return to original size and color after reswelling in water at 23 °C for 60 min. This observation proves that the formation of the dense and collapsed polymer outermost layer of GO-PNIPAM disks are reversible. Also, the observed deswelling ratios agree with the values shown in Fig. 2c upon abrupt heating. Such controllable composition-dependent deswelling behaviors offer opportunities for the precise control of transport and release of functional compounds as well as of shape morphing systems.

To explore the photothermal effect of GO, we characterized the light-responsive properties of GO-PNIPAM composite hydrogels by illuminating UV light (365 nm). GO-PNIPAM thin sheets were prepared in 7.5 cm × 0.5 cm size with 1 mm thickness. UV/vis spectroscopy was used to measure the light absorbances as a function of the wavelength of the GO-PNIPAM composite hydrogel, PNIPAM hydrogel, GO solution and NIPAM-BIS solution (Fig. S6†). The GO-PNIPAM composite hydrogel showed a similar UV absorbance peak near 350 nm compared with the aqueous GO solution. Thereby, GO-PNIPAM composite hydrogels can provide a similar

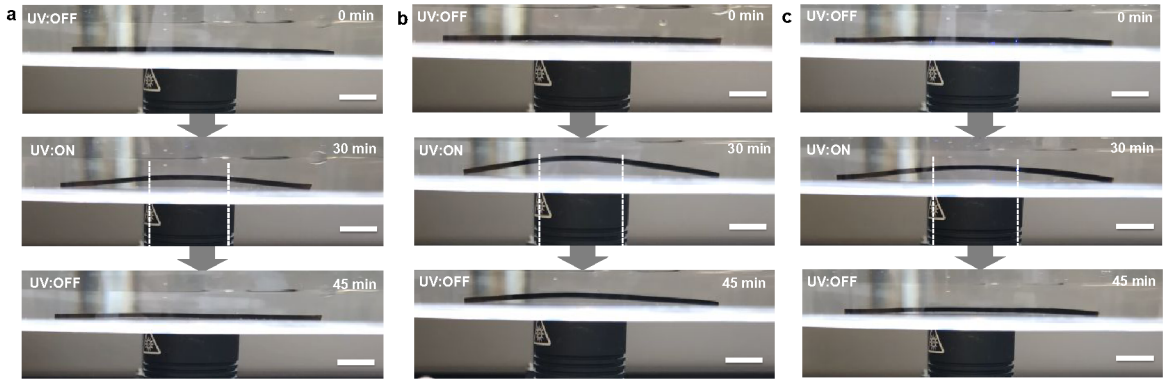

Figure. 5. UV induced photothermal effect causes bending of (a) GO(0.25)-PNIPAM(1); (b) GO(2.5)-PNIPAM(1); (c) GO(6.2)-PNIPAM(1) thin sheets. White dash lines indicate the UV exposing area. UV light is on from 0 to 30 min, and off from 30 to 45 min with the intensity of 160 mW cm^{-2} at 365 nm. Scale bar = 1 cm.

photothermal effect as GO dispersed in a solution. A UV light (Jaxman, U1) was placed close to the GO-PNIPAM sheets so that a central region of the samples was only exposed by UV light with the exposure area of 4.5 cm^2 as shown in Fig. 5. Three hydrogel thin sheets with different GO concentrations, GO(0.25)-PNIPAM(1) (Fig. 5a), GO(2.5)-PNIPAM(1) (Fig. 5b) and GO(6.2)-PNIPAM(1) (Fig. 5c) were illuminated by UV light with the intensity of 160 mW cm^{-2} at 365 nm for 30 min. The composite hydrogel sheets bent toward the light source by the UV irradiation. The GO-PNIPAM sheets were re-swelled in water after turning off UV exposure for 15 min. The shape recovery of sheets from bent to the flat state was observed. The actuation times for *visible bending*, the deflection between the substrate and the bottom surface of GO-PNIPAM hydrogel sheet exceeds 1 mm, of GO(0.25)-PNIPAM(1), GO(2.5)-PNIPAM(1) and GO(6.2)-PNIPAM(1) composite hydrogels were 90, 60 and 30 sec, respectively. The actuation time for *visible bending* decreases with increasing GO loading since higher GO concentration generates relatively more heat. However, as the GO concentration increases from 0.25, 2.5 to 6.2 mg mL^{-1}, the curvatures of bent hydrogel sheets were 0.41, 0.45 and 0.42 cm^{-1}, respectively. This result exhibits the influence of GO on the mechanical properties of GO-PNIPAM samples. Since the elastic bending energy of hydrogel is proportional to its Young's modulus,[53] a higher concentration of GO strengthens Young's modulus thus reduces the degree of bending of the composite hydrogels although the higher concentration of GO could generate more heat (Table S4†). To further explore the mechanical property of GO-PNIPAM, we characterized Young's moduli of GO-PNIPAM with different concentrations of GO and BIS by nanoindentation in the swelled state (Table S5†). The results show Young's modulus of GO-PNIPAM significantly increases with increasing GO concertation due to the high Young's modulus of GO (380 - 470 GPa)[54] and the contribution to the degree of crosslinking density of GO-PNIPAM networks. Therefore, the quantitative analysis of light-driven photothermal deformation should be estimated by the balance between photothermal efficiency and mechanical property for a certain composition of GO-PNIPAM systems. These correlations render great potential to design complex shape morphing by lateral (*e.g.*, 2D patterning) or vertical (*e.g.*, multi-layer structure) variations of the concentrations of GO and BIS thus the degree of swelling/deswelling and Young's modulus. We note that GO(2.5)-PNIPAM(1) and GO(6.2)-PNIPAM(1) (Fig. 5b and c) are still slightly bent after 15 min recovering, not returning to a flat state. Once we manually detached and reloaded both ends of the GO-PNIPAM sheet from the substrate, the sheet became flat within 5 min. It indicates that the friction on the edge of the thin sheets acted as the counterforce to recover to the initial flat state. To convince that their bending was actuated by photothermal heat generation, not by heat from UV exposure itself, a GO(0)-PNIPAM(1) thin sheet was exposed by UV under the same condition. There was no bending observed (Fig. S7a†), and the temperature within the exposing area was not increased above the LCST (~ 33 °C) of PNIPAM (Fig. S7b†). These results prove the bending of GO-PNIPAM thin sheet is actuated due to the heat generation by the photothermal effect of GO, not by the heat from UV lamp.

Conclusions

In summary, we have demonstrated the tunable degree of swelling and deswelling in GO-PNIPAM composite hydrogels by controlling their internal microstructures and the rate of cooling and heating. PNIPAM chains were chemically crosslinked by BIS and physically crosslinked by hydrogen bonding with GO additives, where the concentrations of BIS and GO determine the internal microstructures that can control the swelling and deswelling behaviors. At relatively high BIS but low GO concentrations, much faster diffusion of heat than water

through PNIPAM hydrogels resulted in the formation of the dense and collapsed polymer outermost layer of GO-PNIPAM composite hydrogels, thereby the deswelled sample exhibits no noticeable shrinkage in size (*i.e.*, $\lambda_d > 1$). However, the high loading concentration of GO (> 2.5 mg mL^{-1}) effectively prevents the formation of such dense outermost layer upon abrupt heating, allowing water to be expelled from the sample while deswelling. Since the photothermal property of GO is well preserved in GO-PNIPAM composite hydrogel systems, UV irradiation can lead to the deswelling, thus actuate the shape deformation of GO-PNIPAM thin sheets. We anticipate that this tunable swelling and deswelling of stimuli-responsive composite hydrogels will be useful for programming the transport and release of functional compounds and shape deformation as well as for applications in multiple stimuli-responsive actuators, sensors, biomedical devices, and biomimetic systems.

Conflicts of interest

There are no conflicts to declare.

Acknowledgements

J.B. acknowledges the University of California San Diego (UCSD) start-up funds. Part of this work was performed at the San Diego Nanotechnology Infrastructure (SDNI) of UCSD, a member of the National Nanotechnology Coordinated Infra-structure (NNCI), which is supported by the National Science Foundation (Grant ECCS-1542148). The authors also thank Prof. Karen Christman for allowing us to use a freeze-dryer in her laboratory.

References

E. Ruel-Gariepy and J. C. Leroux, *Eur. J. Pharm. Biopharm.*, 2004, 58, 409-426.

A. Richter, G. Paschew, S. Klatt, J. Lienig, K. F. Arndt and H. P. Adler, *Sensors*, 2008, 8, 561-581.

R. V. Kulkarni and S. Biswanath, *J. Appl. Biomater. Biomech.*, 2007, 5, 125-139.

J. Hu, H. Meng, G. Li and S. I. Ibekwe, *Smart Mater. Struct.*, 2012, 21.

Y.-L. Zhao and J. F. Stoddart, *Langmuir*, 2009, 25, 8442-8446.

S.-k. Ahn, R. M. Kasi, S.-C. Kim, N. Sharma and Y. Zhou, *Soft Matter*, 2008, 4.

W. Deng, H. Yamaguchi, Y. Takashima and A. Harada, *Angew. Chem., Int. Ed. Engl.*, 2007, 46, 5144-5147.

N. A. Peppas and D. S. Van Blarcom, *J. Controlled Release*, 2016, 240, 142-150.

L. Ionov, *Langmuir*, 2015, 31, 5015-5024.

R. Kempaiah and Z. Nie, *J. Mater. Chem. B*, 2014, 2, 2357-2368.

Y. Takashima, S. Hatanaka, M. Otsubo, M. Nakahata, T. Kakuta, A. Hashidzume, H. Yamaguchi and A. Harada, *Nat. Commun.*, 2012, 3, 1270.

S. Furyk, Y. Zhang, D. Ortiz-Acosta, P. S. Cremer and D. E. Bergbreiter, *J. Polym. Sci., Part A: Polym. Chem.*, 2006, 44, 1492-1501.

V. Y. Grinberg, A. S. Dubovik, D. V. Kuznetsov, N. V. Grinberg, A. Y. Grosberg and T. Tanaka, *Macromolecules*, 2000, 33, 8685-8692.

Y. Zhang, S. Furyk, L. B. Sagle, Y. Cho, D. E. Bergbreiter and P. S. Cremer, *J. Phys. Chem. C*, 2007, 111, 8916-8924.

M. Heskins and J. E. Guillet, *J. Macromol. Sci., Chem.*, 1968, 2, 1441-1455.

E. Lee, D. Kim, H. Kim and J. Yoon, *Sci. Rep.*, 2015, 5, 15124.

A. W. Hauser, A. A. Evans, J. H. Na and R. C. Hayward, *Angew. Chem., Int. Ed. Engl.*, 2015, 54, 5434-5437.

J. H. Na, A. A. Evans, J. Bae, M. C. Chiappelli, C. D. Santangelo, R. J. Lang, T. C. Hull and R. C. Hayward, *Adv. Mater.*, 2015, 27, 79-85.

X. Huang, S. Neretina and M. A. El-Sayed, *Adv. Mater.*, 2009, 21, 4880-4910.

X. Zhang, C. L. Pint, M. H. Lee, B. E. Schubert, A. Jamshidi, K. Takei, H. Ko, A. Gillies, R. Bardhan, J. J. Urban, M. Wu, R. Fearing and A. Javey, *Nano Lett.*, 2011, 11, 3239-3244.

R. Hernandez and C. Mijangos, *Macromol. Rapid Commun.*, 2009, 30, 176-181.

H. P. Cong, X. C. Ren, P. Wang and S. H. Yu, *Sci. Rep.*, 2012, 2, 613.

D. Kim, H. S. Lee and J. Yoon, *RSC Adv.*, 2014, 4, 25379-25383.

K. Shi, Z. Liu, Y. Y. Wei, W. Wang, X. J. Ju, R. Xie and L. Y. Chu, *ACS Appl. Mater. Interfaces*, 2015, 7, 27289-27298.

X. Peng, T. Liu, C. Jiao, Y. Wu, N. Chen and H. Wang, *J. Mater. Chem. B*, 2017, 5, 7997-8003.

C.-H. Zhu, Y. Lu, J. Peng, J.-F. Chen and S.-H. Yu, *Adv. Funct. Mater.*, 2012, 22, 4017-4022.

Y. Qiu and K. Park, *Adv Drug Deliv Rev*, 2001, 53, 321-339.

X. He, M. Aizenberg, O. Kuksenok, L. D. Zarzar, A. Shastri, A. C. Balazs and J. Aizenberg, *Nature*, 2012, 487, 214-218.

C. Ma, X. Le, X. Tang, J. He, P. Xiao, J. Zheng, H. Xiao, W. Lu, J. Zhang, Y. Huang and T. Chen, *Adv. Funct. Mater.*, 2016, 26, 8670-8676.

D. R. Dreyer, S. Park, C. W. Bielawski and R. S. Ruoff, *Chem. Soc. Rev.*, 2010, 39, 228-240.

Y. Zhu, S. Murali, W. Cai, X. Li, J. W. Suk, J. R. Potts and R. S. Ruoff, *Adv. Mater.*, 2010, 22, 3906-3924.

J. Y. Luo, L. J. Cote, V. C. Tung, A. T. L. Tan, P. E. Goins, J. S. Wu and J. X. Huang, *J. Am. Chem. Soc.*, 2010, 132, 17667-17669.

K. Wang, J. Ruan, H. Song, J. Zhang, Y. Wo, S. Guo and D. Cui, *Nanoscale Res. Lett.*, 2011, 6, 8.

J. Kim, L. J. Cote, F. Kim, W. Yuan, K. R. Shull and J. X. Huang, *J. Am. Chem. Soc.*, 2010, 132, 8180-8186.

F. Kim, L. J. Cote and J. Huang, *Adv. Mater.*, 2010, 22, 1954-1958.

D. Kim, E. Lee, H. S. Lee and J. Yoon, *Sci. Rep.*, 2015, 5, 7646.

Z. Chen, R. Cao, S. Ye, Y. Ge, Y. Tu and X. Yang, *Sens. Actuators, B*, 2018, 255, 2971-2978.

J. Qi, W. Lv, G. Zhang, F. Zhang and X. Fan, *Polym. Chem.*, 2012, 3.

A. GhavamiNejad, S. Hashmi, H. I. Joh, S. Lee, Y. S. Lee, M. Vatankhah-Varnoosfaderani and F. J. Stadler, *Phys.Chem.Chem.Phys.*, 2014, 16, 8675-8685.

X. H. Wang, X. P. Qiu and C. Wu, *Macromolecules*, 1998, 31, 2972-2976.

X. Z. Zhang, D. Q. Wu and C. C. Chu, *J. Polym. Sci., Part B: Polym. Phys.*, 2003, 41, 582-593.

X. Y. Lin, X. Shen, Q. B. Zheng, N. Yousefi, L. Ye, Y. W. Mai and J. K. Kim, *Acs Nano*, 2012, **6**, 10708-10719.

X. Shen, X. Lin, N. Yousefi, J. Jia and J.-K. Kim, *Carbon*, 2014, **66**, 84-92.

A. D. Ugale, L. Chi, M.-K. Kim, S. Chae, J.-Y. Choi and J.-B. Yoo, *RSC Advances*, 2019, **9**, 4198-4202.

O. Kuksenok and A. C. Balazs, *Adv. Funct. Mater.*, 2013, 23, 4601-4610.

J. Yoon, S. Cai, Z. Suo and R. C. Hayward, *Soft Matter*, 2010, 6.

N. Kato and F. Takahashi, *Bull. Chem. Soc. Jpn.*, 1997, 70, 1289-1295.

R. Yoshida, K. Uchida, Y. Kaneko, K. Sakai, A. Kikuchi, Y. Sakurai and T. Okano, *Nature*, 1995, 374, 240.

R. Yoshida, K. Sakai, T. Okano, Y. Sakurai, B. You Han and K. Sung Wan, *J. Biomater. Sci., Polym. Ed.*, 2012, 3, 155-162.

T. G. Park and A. S. Hoffman, *J. Appl. Polym. Sci.*, 1994, 52, 85-89.

H. W. Kang, Y. Tabata and Y. Ikada, *Biomaterials*, 1999, 20, 1339-1344.

H. G. Schild and D. A. Tirrell, J. Phys. Chem., 1990, 94, 4352-4356.

J. Bae, N. P. Bende, A. A. Evans, J.-H. Na, C. D. Santangelo and R. C. Hayward, *Mater. Horiz.*, 2017, 4, 228-235.

L. Liu, J. Zhang, J. Zhao and F. Liu, *Nanoscale*, 2012, 4, 5910-5916.

GRAPHICAL ABSTRACT

Swelling and deswelling behaviors of graphene oxide-poly(N-isopropylacrylamide) composite hydrogels can be tuned by the concentrations of chemical crosslinker and graphene oxide, and the rate of external temperature change.